Industrial Chemistry & Materials

ROYAL SOCIETY OF CHEMISTRY

PAPER

View Article Online
View Journal | View Issue

Cite this: *Ind. Chem. Mater.*, 2025, **3**, 587

Synthesis and properties of a novel perfluorinated polyimide with high toughness, low dielectric constant and low dissipation factor†

Hangqian Wang,[ab] Yao Zhang,[a] Xialei Lv,*[a] Jinhui Li,*[a] Kuangyu Wang,[a] Guoping Zhang[a] and Rong Sun[a]

With the development of high-frequency communication technologies, polyimide (PI) materials with a low dielectric constant (D_k) and low dissipation factor (D_f) are urgently needed to reduce signal crosstalk and other transmission problems. The introduction of a trifluoromethyl group is a common strategy to reduce D_k and D_f, but the bulky trifluoromethyl group would diminish stacking density and consequently lead to inferior mechanical properties. Herein, a novel diamine monomer, 2,3,4,5,6-pentafluororo-3,5-bis(4-aminophenoxy)-1,1-biphenyl (5FBODA), was designed and synthesized using simple reactions. Subsequently, fluorinated diamine and dianhydride were copolymerized with 5FBODA to obtain a series of fluorinated polyimide (FPI) with excellent dielectric properties and good mechanical performances, particularly high elongation at break. The pentafluorophenyl side group showed an obvious electron-withdrawing effect and made the charge of the structure more balanced, which reduced the molecular polarization rate and charge concentration to some extent, significantly helping in reducing D_k at high frequency. As the 5FBODA content increased, the large lateral group restricted the movement of the main chain, constrained the dipole polarization, thereby effectively diminishing their D_f. Moreover, when 20–30% 5FBODA was added, the pentafluorophenyl side group increased the intermolecular forces, thereby enhancing the elongation at break while maintaining good thermal properties. These FPIs exhibited remarkable advantages for advanced microelectronic packaging applications, providing an innovative solution for the development of next-generation high-performance electronic materials.

Received 7th April 2025,
Accepted 14th May 2025

DOI: 10.1039/d5im00048c

rsc.li/icm

Keywords: Wafer level packaging; Fluorinated polyimide; Low dielectric; High toughness.

1 Introduction

Polyimide (PI), a category of high-performance polymers, has a crucial position in high-end technology fields,[1] including aerospace,[2,3] microelectronics,[4,5] and flexible displays,[6,7] by virtue of its remarkable thermal stability, mechanical strength, and chemical resistance. In particular, PI is extensively utilized as a redistribution layer (RDL) material in wafer-level packaging owing to its outstanding comprehensive performance.[8] However, as electronic devices continue to evolve toward miniaturization, higher speed and higher frequency, the high dielectric constant (D_k) and dissipation factor (D_f) of conventional PI have become key limiting factors restricting their further advancement in advanced applications.[9–13] Therefore, developing new polyimide materials with low D_k and D_f and excellent mechanical properties has become one of the hot spots in the field of materials research.[14–16]

Traditional PIs encounter difficulties in fulfilling the requisites of high-frequency applications. To diminish signal transmission loss, it is essential to acquire PI materials with low D_k and D_f by designing new PI structures.[17–19] The molecular polarizability is a microscopic parameter describing the polarization characteristics of dielectrics. And the dielectric constant is a macroscopic parameter for measuring the polarization ability of dielectrics. Their relationship is as shown in the Clausius–Mosotti equation.[20,21]

$$(\varepsilon_r - 1)/(\varepsilon_r + 2) = \frac{\sum_i N_i \alpha_i}{3\varepsilon_0} \quad (1)$$

where ε_0 is the vacuum permittivity ($\varepsilon_0 = 8.854 \times 10^{-12}$ F m^{-1}), ε_r is the relative permittivity, N_i is the number density (number of particles per unit volume) of the ith particle, and α_i is the polarizability of the particle i. When the molecular

[a] *Shenzhen Institutes of Advanced Electronic Materials, Shenzhen Institutes of Advanced Technology, Chinese Academy of Sciences, Shenzhen 518055, P. R. China. E-mail: xl.lv@siat.ac.cn, jh.li@siat.ac.cn*
[b] *University of Chinese Academy of Sciences, Beijing 100049, P. R. China*
† Electronic supplementary information (ESI) available. See DOI: https://doi.org/10.1039/d5im00048c

weight of the dielectric is M, density is ρ, molar polarization strength is P_M and the molar volume is V_M, and considering $V_M = M/\rho$, then

$$\varepsilon_r = \frac{1 + 2\frac{P_M}{V_M}}{1 - \frac{P_M}{V_M}} \quad (2)$$

Thus, the dielectric constant of PI can be reduced by lowering the P_M/V_M value of the molecular structure. The introduction of the F element is capable of effectively decreasing the molecular polarizability (P_M), resulting in a low D_k of PI. This can be ascribed to the large electronegativity (4.0) of the F element.[22–24] Such high electronegativity enables the nucleus to tightly attract extra-nuclear electrons, giving rise to high C–F bonding energy and small electronic polarizability. Mitsuru Ueda *et al.*[25] obtained fluorinated diamine monomers through a five-step organic synthesis procedure, and further polymerized them with pyromellitic dianhydride (PMDA) to obtain fluorinated PIs *via* thermal imidization, which showed a D_k of 2.65 at 1 MHz calculated from the average refractive index. The addition of perfluorobiphenyl units along with phenylene ether units into the main chains of polyimides effectively lowers the D_k while preserving their thermal stability. In addition, a greater portion of the research effort has focused on the introduction of trifluoromethyl groups into the side chains to reduce the D_k of PIs. Huang *et al.*[26] prepared three aromatic rigid fluorinated diamines and polymerized them with 1,2,4,5-cyclohexanetetracarboxylic dianhydride (CHDA) and 4,4′-(hexafluoroisopropylidene)diphthalic anhydride (6FDA) *via* one- or two-step polycondensation reactions to obtain fluorinated PIs. These fluorinated PIs exhibited D_k ranging from 2.81 to 3.35 and D_f ranging from 0.0047 to 0.0232 at 10 GHz. Peng *et al.*[27] designed and synthesized a series of PIs containing perfluorocyclobutyl (FPCB) aryl ether groups. The introduction of PFCB disrupted the electron-conjugated structure and elongated the length of the repeating unit, leading to a low dipole moment. Meanwhile, it exhibited a lower chain stacking density, which significantly decreased the dielectric constant of the PIs. However, the lower chain stacking density gave rise to a weaker intermolecular force, which was detrimental to the mechanical properties of the PIs and further restricted their application in advanced packaging.

In this report, as shown in Fig. 1, a diamine, namely 2,3,4,5,6-pentafluoro-3,5-bis(4-aminophenoxy)-1,1-biphenyl (5FBODA), possessing pentafluorobenzene units on the side chain, was designed and synthesized to lower the dielectric properties of PI at 10 GHz. (Perfluoropropane-2,2-diyl)bis(4,1-phenylene)bis(1,3-dioxo-1,3-dihydroisobenzo-furan-5-carboxylate) (6FESDA), which contains two trifluoromethyl groups, was selected as the dianhydride to participate in the reaction. Furthermore, another diamine also containing two trifluoromethyl groups, 2,2-bis[4-(4-

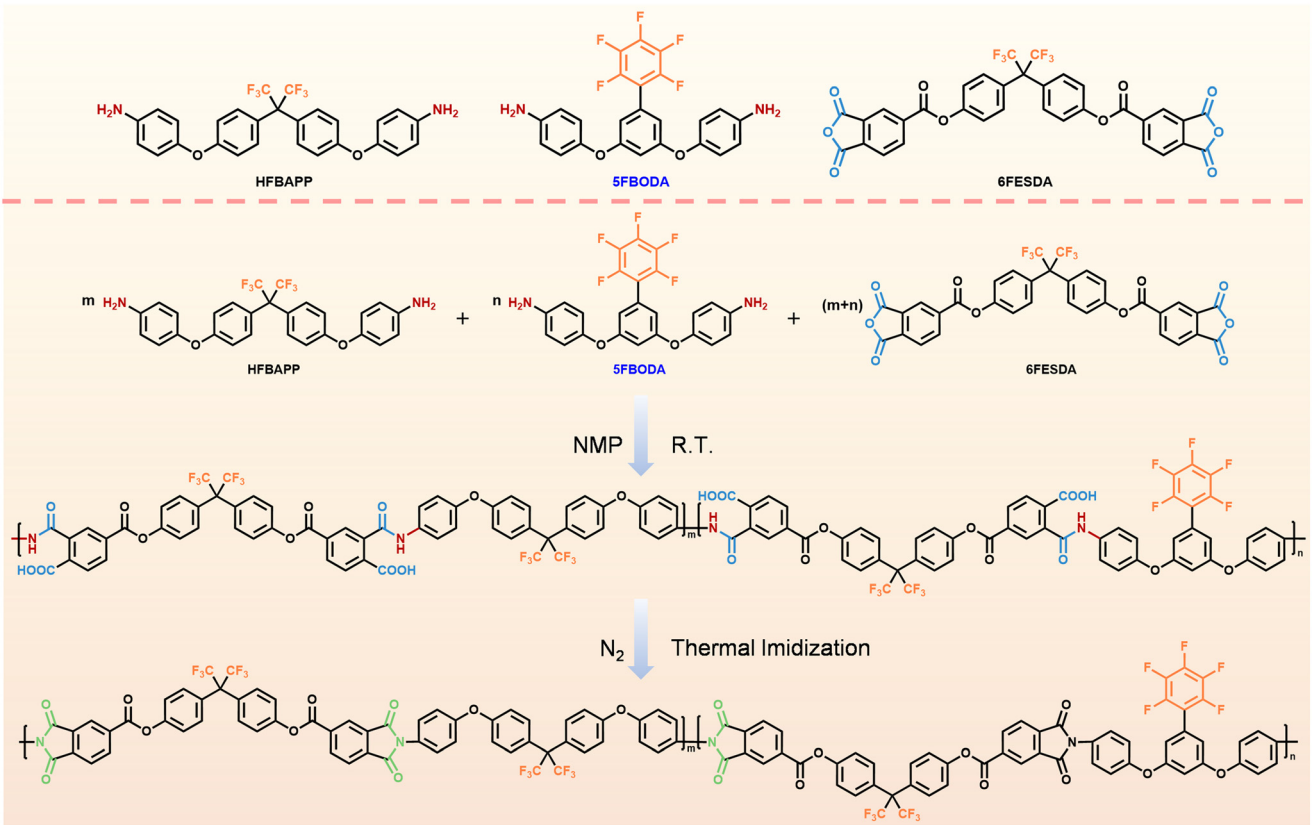

Fig. 1 Schematic of the preparation process of fluorinated polyimides.

aminophenoxy)phenyl]-1,1,1,3,3,3-hexafluoropropane (HFBAPP), was introduced and co-polymerized with 5FBODA and 6FESDA to prepare a series of FPIs. The strong electron-withdrawing effect of pentafluorobenzene on the side chains effectively reduced the charge density of the polyimide groups, thus achieving lower dielectric properties. On the other hand, when the ratio of 5FBODA increased, it restricted the movement of the main chain, further constraining the dipole polarization and effectively diminishing its D_f. Additionally, the flexible ether bonds and intermolecular interactions within the molecule contributed to improving the elongation at break (ε_b). Among them, FPI-3 demonstrated the best overall performance (D_k = 2.60, D_f = 3.37 × 10^{-3}, ε_b = 50.1%) and showed considerable potential for application in advanced packaging.

2 Results and discussion

2.1 Molecular weight analysis

The molecular weights of the synthesized fluorinated poly (amic acid) (FPAA) were characterized by Gel Permeation Chromatography (GPC) (Table S1†). The results demonstrated that the number average molecular weight (M_n) and weight average molecular weight (M_w) of FPAA were within the ranges of 58 543–74 078 g mol^{-1} and 74 457–91 822 g mol^{-1}, respectively. The molecular weight of FPAA decreased with the increase of the content of 5FBODA. The fluorine atom on the side group of the 5FBODA molecule exerted a strong electron-withdrawing effect, which weakened the electron-giving ability of the amine group to a certain extent, thus reducing the reactivity.

2.2 X-ray diffraction analysis

The molecular chain spacing of the synthesized FPI was characterized using X-ray diffraction (XRD), and as demonstrated in Fig. 2a, FPIs lacked obvious diffraction peaks, indicating an amorphous structure. As presented in Table S2,† the 2θ range of FPI was 14.54–15.99°, and the corresponding interplanar spacing was calculated from the Bragg equation and ranged from 5.54 to 6.09 Å. The interplanar spacing of FPIs exhibited an increasing trend with the increase in 5FBODA, which might be attributed to the fact that the increasing bulky pentafluorophenyl group of 5FBODA introduces a greater amount of free volume.

2.3 ATR-FTIR analysis

The structures of FPIs were characterized using Attenuated Total Reflectance-Fourier Transform Infrared Spectroscopy (ATR-FTIR), and the resulting spectra are depicted in Fig. 2b. It can be seen that the absorption peaks at 1780 cm^{-1} and 1720 cm^{-1} were, respectively, ascribed to the asymmetric and symmetric stretching vibrations of the C═O bond. Moreover, the C–N stretching peak within the acylimide ring was observed at 1380 cm^{-1}, whereas the peak at 720 cm^{-1} was attributed to the bending vibration of the C═O bond. In addition, the –C–O–C– stretching vibrational peak presented in the molecular structure was detected at 1210 cm^{-1}, and the vibrational peak of the benzene ring was observed at 1500 cm^{-1}. The characteristic peaks corresponding to the trifluoromethyl group were observed at 1225 cm^{-1} and 1170 cm^{-1}. The characteristic peak representing the C–F bond of 5FBODA was observed at a wavelength of 1480 cm^{-1}. In summary, the infrared spectra

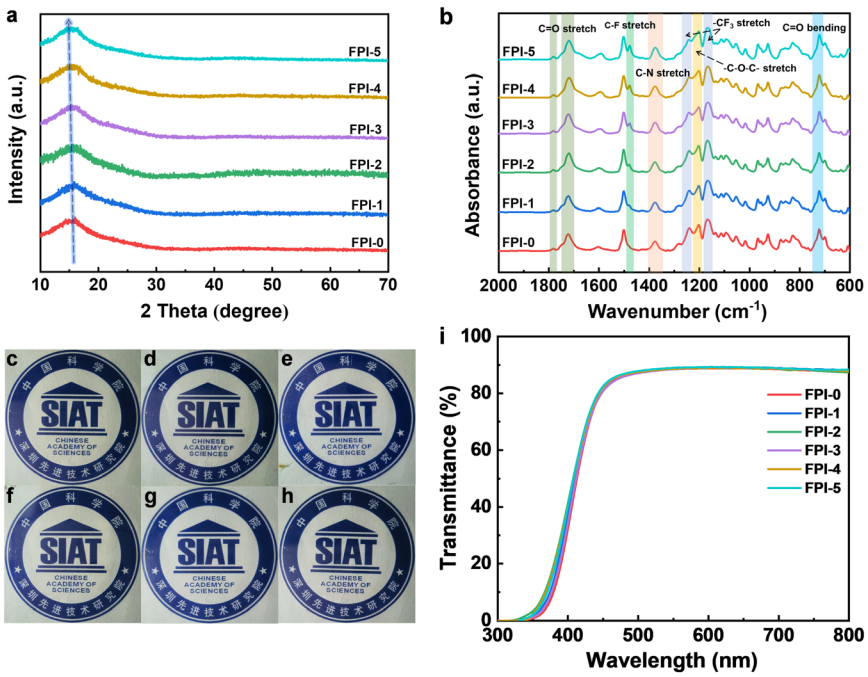

Fig. 2 (a) XRD spectrum of FPIs; (b) ATR-FTIR spectrum of FPIs; (c)–(h) photographs of FPI-0-5; and (i) UV transmission curve of FPIs.

provide convincing evidence of the successful synthesis of FPIs.

2.4 Optical properties

As shown in Fig. 2c–h, all FPIs exhibit good optical transparency. To further explore the optical properties, the UV transmission curves were characterized through ultraviolet-visible spectrum (UV-vis) (Fig. 2i). The transmittance values at 450 nm (T_{450}), 500 nm (T_{500}) and 550 nm (T_{550}) for FPIs ranged from 80.8% to 82.4%, 87.1% to 87.9% and 88.5% to 89.0%, respectively (Table S2†). The optical differences among them were not substantial, indicating that the presence of the pentafluorophenyl side group in the 5FBODA monomer had a similar influence on the charge transfer complex (CTC) effect of the molecular chain as the hexafluoropropyl group in HFBAPP.

2.5 Thermal properties

The thermal decomposition temperature of FPI was determined by thermal gravimetric analysis (TGA) (Fig. 3a). The temperatures at 5% weight loss ($T_{d,5\%}$) and 10% weight loss ($T_{d,10\%}$) of FPIs were within the ranges 437–472 °C and 460–501 °C, respectively (Fig. 3d and e and Table 1). Even at 800 °C, the carbon residual, denoted as R800, of FPIs remained above 50% (Table 1). These results indicate that these FPIs exhibit relatively good thermal stability. In addition, the thermal stability of the FPI film slightly decreased as the content of 5FBODA monomer was increased. This was due to the number of benzene ring units in the main chain of 5FBODA being lower than that of HFBAPP. Additionally, a faster rate of thermal weight loss was observed for the FPI within the temperature range of 400 to 600 °C, which might be attributed to the breakage and decomposition of the C–F bond in the pentafluorophenyl group of 5FBODA.[28]

The glass transition temperatures (T_g) of FPIs were tested by differential scanning calorimetry (DSC), as shown in Fig. 3c. The T_g of FPIs were in the range of 221.3 °C to 240.0 °C (Fig. 3f and Table 1). Among them, the T_g of FPIs exhibited a general tendency of first decreasing and then increase with increasing 5FBODA content. When the 5FBODA content was less than 30%, T_g decreased as the 5FBODA content increased. This result corresponded to an

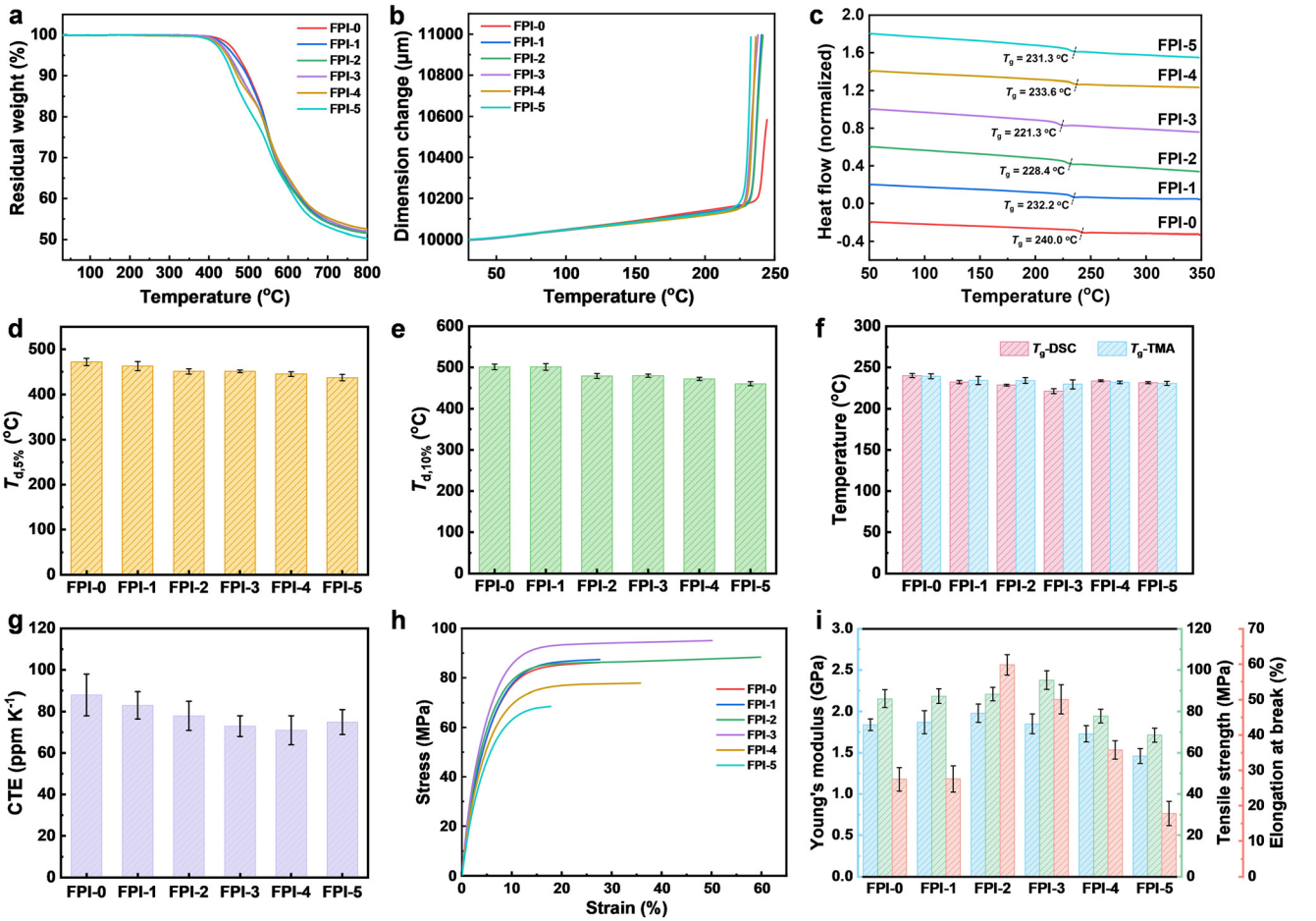

Fig. 3 Thermal and mechanical properties of FPIs. (a) TGA curves; (b) TMA curves; (c) DSC curves; (d) temperature at 5% weight loss ($T_{d,5\%}$); (e) temperature at 10% weight loss ($T_{d,10\%}$); (f) glass transition temperatures; (g) coefficient of thermal expansion; (h) DMA stretch curve; and (i) mechanical parameters of FPIs.

Table 1 Thermal and mechanical properties of FPIs

Number of FPIs	$T_{d,5\%}$ °C	$T_{d,10\%}$ °C	R_{800} %	T_g (DSC) °C	T_g (TMA) °C	CTE[a] ppm K^{-1}	σ_{max} MPa	ε_b %	E GPa
FPI-0	472	501	51.7	240.0	239.1	88	86.2 ± 4.3	27.5 ± 3.3	1.84 ± 0.07
FPI-1	463	501	51.5	232.2	234.1	83	87.4 ± 3.5	27.6 ± 3.7	1.87 ± 0.14
FPI-2	451	479	51.5	228.4	234.0	79	88.4 ± 3.2	59.8 ± 2.9	1.98 ± 0.11
FPI-3	451	480	51.9	221.3	229.4	73	95.1 ± 4.5	50.1 ± 4.1	2.18 ± 0.12
FPI-4	445	472	52.5	233.6	231.8	71	77.8 ± 3.4	35.8 ± 2.6	1.73 ± 0.10
FPI-5	437	460	50.8	231.3	230.4	75	68.5 ± 3.4	17.8 ± 3.5	1.46 ± 0.09

[a] Temperature range: 50–200 °C.

increase in the *d*-spacing observed in the XRD patterns (Fig. 2a and Table S2†). This suggested that the introduction of pentafluorophenyl groups increased the free volume and reduced the packing density of the molecular chains, thereby decreasing T_g. However, When the molar content of pentafluorophenyl groups exceeded 30%, the bulky side group restricted the mobility of the molecular chains, resulting in a subsequent increase in T_g.[29,30] In addition, the T_g values of FPIs were also tested by thermomechanical analysis (TMA) (Fig. 3b), and the trend was consistent with that tested by DSC. The coefficient of thermal expansion (CTE) of FPIs ranged from 71 to 88 ppm K^{-1} and decreased with the increase of 5FBODA monomer (Fig. 3g and Table 1). This result may be explained by the fact that 5FBODA was beneficial for increasing the molecular rigidity.

2.6 Mechanical properties

The mechanical properties of FPIs were tested by dynamic mechanical analysis (DMA) (Fig. 3h and i). Among them, FPI-2 and FPI-3 exhibited excellent mechanical properties, especially the elongation at break, as high as 59.8% and 50.1%, which was superior to most of the fluorinated PI films in reported literature (Table S3†).[26,31–35] Based on the DMA curves, the values of maximum tensile strength (σ_{max}), elongation at break (ε_b) and modulus (E) were calculated in the range of 68.5 to 95.1 MPa, 17.8 to 59.8% and 1.46 to 2.18 GPa, respectively (Table 1). With the increase in 5FBODA, the mechanical properties of FPIs first increased and then decreased, demonstrating that 5FBODA increased the intermolecular forces at low content, consequently leading to an increase in the σ_{max} and E values. In addition, the flexible ether bonds present in HFBAPP and 5FBODA also improved the elongation at break of FPI. However, when the 5FBODA molar content exceeded 30%, the mechanical properties were noticeably diminished. This might be because the excessively large volume of 5FBODA with pentafluorobenzene side groups obstructs the movement of the molecular chains, thereby decreasing the mechanical properties of FPI-4 and FPI-5.

2.7 Dielectric properties

The dielectric properties of PI films at high frequency (10 GHz) were investigated using a vector network analyzer, and the results are summarized in Fig. 4a and Table 2. Significantly, the D_k of FPI-3 was as low as 2.60, while the D_f was 3.37 × 10^{-3}, which was compared to the excellent materials reported (Table S4†). The introduction of a small amount of fluorinated groups would reduce the overall polarizability and orientation polarization ability of the molecule, and the dielectric constant would first decrease.[36–38] However, further excessive fluorinated groups might lead to an increase of polar group density, a significant increase in electronic polarization contribution; therefore, an increase in dielectric constant was seen.[23,39,40] Furthermore, to clarify the influence of structure on dielectric properties, the theoretical calculation of the electronic cloud distribution of diamine monomers was carried by density functional theory (DFT) with the Gaussian 16 software in a B3LYP

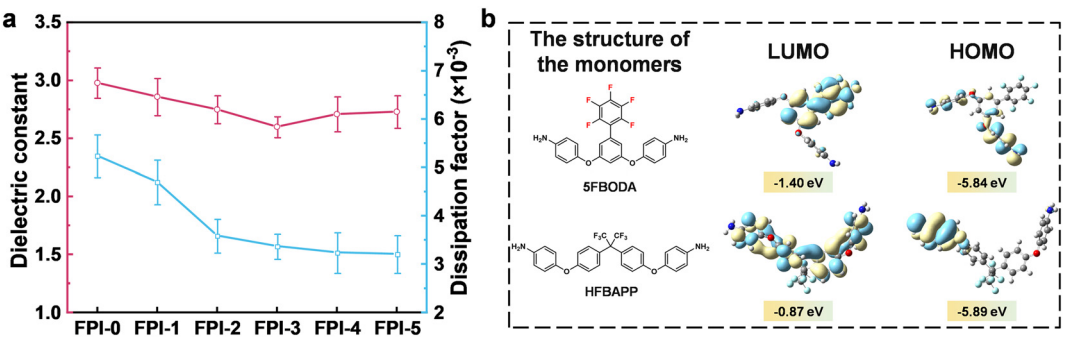

Fig. 4 (a) Dielectric properties of FPIs; (b) LUMO and HOMO energy values of 5FBODA and HFBAPP.

Table 2 Dielectric properties and hydrophobicity of FPIs

Number of FPIs	Dielectric properties[a]		Hydrophobicity
	D_k	D_f ($\times 10^{-3}$)	WA (%)
FPI-0	2.98 ± 0.13	5.24 ± 0.44	0.37
FPI-1	2.86 ± 0.16	4.70 ± 0.46	0.39
FPI-2	2.75 ± 0.12	3.59 ± 0.35	0.43
FPI-3	2.60 ± 0.09	3.37 ± 0.26	0.48
FPI-4	2.71 ± 0.15	3.24 ± 0.42	0.51
FPI-5	2.73 ± 0.14	3.21 ± 0.39	0.53

[a] Tested at 10 GHz, room temperature.

approach and the 6-31G basis set,[41–43] as shown in Fig. 4b. The calculation results demonstrated that the pentafluorobenzene of 5FBODA had a strong electron-withdrawing effect, which decreased the intrinsic dipole moment of the imide group and effectively reduced the D_k of FPIs at high frequency.[44,45] The D_f showed a continuously decreasing trend with the content of 5FBODA. When the ratio of 5FBODA increased, the movement of the main chain was restricted, which further constrained the dipole polarization and effectively diminished its D_f.[46]

2.8 Hydrophobic and solubility properties

The water absorption (WA) values of FPIs were measured using a published method,[41,47] and the values ranged from 0.37% to 0.53% (Table 2). The WA value of FPIs decreased continuously as the content of 5FBODA increased. There existed a significant positive correlation between water absorption and the molecular chain spacing of FPIs (as seen in Table S1†).

As the content of 5FBODA increased, the solubility of FPI became greater (as shown in Table S5†). This result was attributed to the spatial steric hindrance effect of the side groups in 5FBODA. Among them, the solubility of FPIs in polar non-protonic solvents was increased, and FPI-5 exhibited the best solubility due to possessing the highest number of pentafluorophenyl side ratios of 5FBODA. Moreover, all FPIs were soluble in *N*-methyl-2-pyrrolidone (NMP), which indicated that FPIs synthesized through thermal imidization possessed good processability.

3 Conclusion

A novel fluorinated diamine monomer was successfully synthesized and copolymerized with another fluorinated diamine and dianhydride to fabricate fluorinated polyimide films. These FPI films exhibit remarkable dielectric properties, excellent mechanical properties, good thermal stability, and satisfactory solubility and hydrophobicity. Among these FPI films, FPI-3 exhibited excellent properties (D_k = 2.60, D_f = 3.37 × 10^{-3}, WA = 0.48%, $T_{d,5\%}$ = 451 °C, T_g = 221 °C, σ_{max} = 95.1 MPa, ε_b = 50.1%, and E = 2.18 GPa), making it one of the best candidates. Finally, the excellent dielectric properties of FPI films can effectively reduce signal transmission problems, and their high toughness can improve their long-term reliability and processability, offering substantial promise for the advancement of advanced electronic packaging technologies.

4 Experimental section

4.1 Design principles of 5FBODA

5FBODA was synthesized *via* a simple and efficient route. Initially, dinitro intermediates were obtained by performing an aromatic nucleophilic substitution on 5-bromoresorcinol. Subsequently, dinitro intermediates containing pentafluorobenzene were synthesized by incorporating pentafluorobenzene side groups *via* the Suzuki–Miyaura reaction. Eventually, 5FBODA was obtained by hydrogenating 2,3,4,5,6-pentafluoro-3,5-bis(4-nitrophenoxy)-1,1-biphenyl to reduce its nitro groups to amino groups (Fig. S1†).

4.2 Synthesis of fluorinated polyamic acids (FPAAs)

5FBODA (0.23 g, 0.5 mmol) and HFBAPP (2.33 g, 4.5 mmol) were dissolved in 23.9 mL (20 wt%) NMP in a 100 mL three-necked flask under mechanical stirring at room temperature under a nitrogen atmosphere. Subsequently, 6FESDA (1.71 g, 2.5 mmol) was added in two portions and reacted for 24 h (Fig. 1). At the end of the reaction, the air bubbles were removed by centrifugation to obtain a clear and viscous FPAA solution. The remaining FPAAs were prepared in a manner analogous to that employed for FPAA-1, using a total of 5.0 mmol of diamine and 2.5 mmol × 2 of dianhydride. The volume of NMP used ensured that the solid content of the reaction system was 20 wt%. According to the molar ratios of 5FBODA and HFBAPP (0 : 10, 1 : 9, 2 : 8, 3 : 7, 4 : 6, 5 : 5), the FPAAs were named as FPAA-0–FPAA-5, and the corresponding FPIs were named as FPI-0–FPI-5. The FPAA numbers, relevant proportions and masses of 5FBODA, HFBAPP, 6FESDA, and NMP are presented in Table S6.†

4.3 Synthesis of FPIs

The transparent FPAA solutions were spin-coated on 10 × 10 cm clean glass plates and prebaked at 80 °C for 5 min. Then, it was placed in a nitrogen oven and heated to 100 °C at a rate of 5 °C min^{-1}, kept for 1 h. The temperature was increased at the same rate and maintained at 200 °C for 1 h, 300 °C for 1 h, and 350 °C for 1 h. The sample was peeled off from the glass plate in deionized water and dried at 120 °C under vacuum to obtain dry and flat FPI films, named FPI-*n*, where *n* is the number of parts of the 5FBODA monomer in the total molar amount of the diamine.

4.4 Characterization

The synthesized 5FBODA, as well as the intermediates of the organic synthesis process, were characterized by ^{1}H NMR, ^{13}C NMR, and ^{19}F NMR using a nuclear magnetic resonance spectrometer (AVANCE-III-400 MHz, NMR, Bruker Technologies GmbH, Germany). The compounds (~20 mg) were dissolved in 600 μL DMSO-d_6 containing

tetramethylsilane (δ_H = 0.00 ppm) as an internal reference. High-resolution mass spectrometry (Q EXACTIVE, HRMS, ThermoFisher Scientific, Inc., USA) and high-performance liquid chromatography (Ultimate 3000, HPLC, ThermoFisher Scientific, Inc., USA) were used to confirm the molecular weight and purity of the diamine monomer 5FBODA. Infrared spectra were acquired using a Fourier Transform Infrared Spectrometer (Vertex 70, FTIR, Bruker Technology GmbH, Germany) at room temperature, ATR mode with a scan range of 4000–6000 cm^{-1}. The molecular weight and polydispersity of the PAAs were determined by Gel Permeation Chromatography (Alliance e2695, GPC, Shanghai Waters Technology Co. China). The M_n and M_w values were calibrated using a polystyrene standard curve. X-ray diffraction (D8, Advanced, XRD, Bruker Technologies GmbH, Germany) was used to characterize the molecular chain spacing of the PIs. The diffractometer was used to radiate CuKα rays of 0.15418 nm wavelength onto a PI film of about 2 cm × 2 cm size, with 2θ ranging from 10° to 70°, and the interplanar spacing, d, was calculated using Bragg's equation:

$$2d \times \sin\theta = n\lambda$$

where θ is the angle between the incident line, the reflecting line and the reflecting crystal surface, λ is the wavelength and n is the number of reflecting stages. The optical properties of the PIs were tested by ultraviolet visible spectrum (UV-3600, UV-vis, SHIMADZU, Japan). The films were placed on 5 cm × 5 cm clean and transparent glass plates, and an identical glass plate was used as a reference plate.

The thermal stability of the PIs was tested at 30–800 °C using Thermal Gravimetric Analysis (SDT Q6000, TGA, TA Instruments Inc., USA) at a ramp rate of 10 °C min^{-1} in a nitrogen atmosphere. The T_g of the PIs were tested at 30–350 °C using a Differential Scanning Calorimeter (DSC 2500, DSC, TA Instruments Inc., USA) at a ramp rate of 10 °C min^{-1} in a nitrogen atmosphere. The dimensional stability of the PIs and the T_g of the APIs were tested using a thermomechanical analyzer (TMA-SDTA2+, TMA, TA Instruments Inc., USA) from room temperature to 400 °C at a ramp rate of 5 °C min^{-1} under a nitrogen atmosphere. The slope of the dimensional change with temperature from 50 °C to T_g was taken as the CTE, and this parameter was used to express the dimensional stability of the PIs. In this case, since the T_g of the APIs cannot be measured by DSC, it was replaced by the result of the TMA. Specifically, the temperature at the intersection of the tangent lines before and after the sudden change in CTE was the T_g. The D_k and D_f of the PIs were measured using a vector network analyzer (E5071C ENA, VNA, Keysight Technologies, Inc., USA). The corresponding resonator operates at frequency ranges of 1.1/2.5/5/10/15 GHz, with measurement accuracies of ±3% for D_k and ±5% for D_f. The temperature range is from −75 °C to 110 °C. The FPI was prepared as a film with a length of 5 cm, a width of 5 cm, and a thickness ranging from 30 to 34 μm. The films were dried in a vacuum oven at 100 °C for at least 8 h before testing. Thickness of FPIs was measured using a thickness gauge and recorded in the program. The films were then placed in a 10 GHz resonator for testing, and the dielectric performance data were recorded. Each sample was measured at least 5 times, and the average values were obtained after excluding any abnormal data. The temperature and humidity were maintained at 25 °C and 60% RH during testing. The change in mass of 200 mg of dried PI films before and after immersion in deionized water for 24 h was calculated according to the following water absorption equation:

$$WA = (W_b - W_a)/W_a \times 100\%$$

where W_a is the mass of the PI film before immersion and W_b is the mass of the PI film after immersion. The solubility was tested by dissolving 5 mg of PI films in 8 mL of solvent at room temperature for 24 h, and the undissolved film was heated to 60 °C and continued to be observed for 24 h.

Data availability

The data supporting this article have been included as part of the ESI.†

Author contributions

Hangqian Wang: writing – original draft, data curation, conceptualization. Yao Zhang: writing – review & editing, data curation, investigation. Xialei Lv: writing – review & editing, supervision, funding acquisition. Jinhui Li: supervision, methodology, funding acquisition. Kuangyu Wang: methodology. Guoping Zhang: funding acquisition. Rong Sun: funding acquisition.

Conflicts of interest

The authors declare no conflict of interest.

Acknowledgements

This work was supported by the National Natural Science Foundation of China (62304141, 62174170, 62404140), Guangdong Basic and Applied Basic Research (2023A1515010766, 2022B1515120037), Key Area Research and Development program of Guangdong Province (2024B0101120001, 2023B0101030001), Shenzhen Science and Technology Program (20220807020526001), Autonomous deployment project of China National Key Laboratory of Materials for Integrated Circuits (No. NKLJCZ2023-A05), The SIAT Innovation Program for Excellent Young.

References

1 D.-J. Liaw, K.-L. Wang, Y.-C. Huang, K.-R. Lee, J.-Y. Lai and C.-S. Ha, Advanced polyimide materials: Syntheses, physical properties and applications, *Prog. Polym. Sci.*, 2012, **37**, 907–974.

2 S. Flores-Bonano, J. Vargas-Martinez, O. M. Suárez and W. Silva-Araya, Tortuosity index based on dynamic mechanical properties of polyimide foam for aerospace applications, *Materials*, 2019, **12**, 1851.
3 H. Zuo, Y. Chen, G. Qian, F. Yao, H. Li, J. Dong, X. Zhao and Q. Zhang, Effect of simultaneously introduced bulky pendent group and amide unit on optical transparency and dimensional stability of polyimide film, *Eur. Polym. J.*, 2022, **173**, 111317.
4 A. A. Tyuftin and J. P. Kerry, Review of surface treatment methods for polyamide films for potential application as smart packaging materials: Surface structure, antimicrobial and spectral properties, *Food Packag. Shelf Life*, 2020, **24**, 100475.
5 K. H. K. Frank, T.-E. Lin, J. Lin, Y. S. Lin, S. Chen and F. L. Chien, The comparative study of high and low temperature cure polyimide for wafer level package with ultra-thick re-distribution copper layer, *IEEE Electron. Compon. Technol. Conf.*, 2021, **71**, 959–964.
6 S. D. Kim, B. Lee, T. Byun, I. S. Chung, J. Park, I. Shin, N. Y. Ahn, M. Seo, Y. Lee and Y. Kim, Poly (amide-imide) materials for transparent and flexible displays, *Sci. Adv.*, 2018, **4**, eaau1956.
7 X. Xia, X. He, S. Zhang, F. Zheng and Q. Lu, Short-side-chain regulation of colorless and transparent polyamide-imides for flexible transparent displays, *Eur. Polym. J.*, 2023, **191**, 112030.
8 J. Luo, Y. Wu, Y. Sun, G. Wang, Y. Liu, X. Zhao and G. Ding, Preparation and characterization of high thermal conductivity and low CTE polyimide composite reinforced with diamond nanoparticles/SiC whiskers for 3D IC interposer RDL dielectric, *Appl. Sci.*, 1962, **2019**, 9.
9 J. G. Andrews, S. Buzzi, W. Choi, S. V. Hanly, A. Lozano, A. C. K. Soong and J. C. Zhang, What will 5G be?, *IEEE J. Sel. Areas Commun.*, 2014, **32**, 1065–1082.
10 J. H. Lau, M. Li, Q. M. Li, I. Xu, T. Chen, Z. Li, K. H. Tan, Q. X. Yong, Z. Cheng and K. S. Wee, Design, materials, process, fabrication, and reliability of fan-out wafer-level packaging, *IEEE Trans. Compon., Packag., Manuf. Technol.*, 2018, **8**, 991–1002.
11 J. H. Lau, Recent advances and trends in fan-out wafer/panel-level packaging, *J. Electron. Packag.*, 2019, **141**, 040801.
12 A. O. Watanabe, M. Ali, S. Y. B. Sayeed, R. R. Tummala and M. R. Pulugurtha, A review of 5G front-end systems package integration, *IEEE Trans. Compon., Packag., Manuf. Technol.*, 2021, **11**, 118–133.
13 R. Gao, R. Ma, J. Li, M. Su, F. Hou and L. Cao, Selection and characterization of photosensitive polyimide for fan-out wafer-level packaging, *IEEE Trans. Compon., Packag., Manuf. Technol.*, 2021, **12**, 368–374.
14 I. Gouzman, E. Grossman, R. Verker, N. Atar, A. Bolker and N. Eliaz, Advances in polyimide-based materials for space applications, *Adv. Mater.*, 2019, **31**, 1807738.
15 H. Li, F. Bao, X. Lan, S. Li, H. Zhu, Y. Li, M. Wang, C. Zhu and J. Xu, Fluorinated polyimide with triphenyl pyridine structure for 5G communications: Low dielectric, highly hydrophobic, and highly transparent, *Eur. Polym. J.*, 2023, **197**, 112327.
16 C. Zhang, X. He and Q. Lu, Polyimide films with ultralow dielectric loss for 5G applications: Influence and mechanism of ester groups in molecular chains, *Eur. Polym. J.*, 2023, **200**, 112544.
17 Y. Chen, B. Lin, X. Zhang, J. Wang, C. Lai, Y. Sun, Y. Liu and H. Yang, Enhanced dielectric properties of amino-modified-CNT/polyimide composite films with a sandwich structure, *J. Mater. Chem. A*, 2014, **2**, 14118–14126.
18 Y. Li, G. Sun, Y. Zhou, G. Liu, J. Wang and S. Han, Progress in low dielectric polyimide film–a review, *Prog. Org. Coat.*, 2022, **172**, 107103.
19 J.-W. Zha, Y. Tian, M.-S. Zheng, B. Wan, X. Yang and G. Chen, High-temperature energy storage polyimide dielectric materials: polymer multiple-structure design, *Mater. Today Energy*, 2023, **31**, 101217.
20 M. Valiskó and D. Boda, Correction to the Clausius–Mosotti equation: The dielectric constant of nonpolar fluids from Monte Carlo simulations, *J. Chem. Phys.*, 2009, **131**, 164120.
21 H. Chen, B. Tang, C. Zhong, Y. Yuan, Y. Tan and S. Zhang, The dielectric constant and quality factor calculation of the microwave dielectric ceramic solid solutions, *Ceram. Int.*, 2017, **43**, 7383–7386.
22 C.-C. Kuo, Y.-C. Lin, Y.-C. Chen, P.-H. Wu, S. Ando, M. Ueda and W.-C. Chen, Correlating the molecular structure of polyimides with the dielectric constant and dissipation factor at a high frequency of 10 GHz, *ACS Appl. Polym. Mater.*, 2020, **3**, 362–371.
23 X. He, S. Zhang, Y. Zhou, F. Zheng and Q. Lu, The "fluorine impact" on dielectric constant of polyimides: A molecular simulation study, *Polymer*, 2022, **254**, 125073.
24 Y. Zhang, S. Huang, X. Lv, K. Wang, H. Yin, S. Qiu, J. Li, G. Zhang and R. Sun, Polyimides with low dielectric constants and dissipation factors at high frequency derived from novel aromatic diamines with bistrifluoromethyl pendant groups, *Polym. Chem.*, 2023, **14**, 3862–3871.
25 Y. Watanabe, Y. Shibasaki, S. Ando and M. Ueda, Synthesis and characterization of novel low-k polyimides from aromatic dianhydrides and aromatic diamine containing phenylene ether and perfluorobiphenyl units, *Polym. J.*, 2006, **38**, 79–84.
26 F. Bao, H. Lei, B. Zou, W. Peng, L. Qiu, F. Ye, Y. Song, F. Qi, X. Qiu and M. Huang, Colorless polyimides derived from rigid trifluoromethyl-substituted triphenylenediamines, *Polymer*, 2023, **273**, 125883.
27 W. Peng, H. Lei, L. Qiu, F. Bao and M. Huang, Perfluorocyclobutyl-containing transparent polyimides with low dielectric constant and low dielectric loss, *Polym. Chem.*, 2022, **13**, 3949–3955.
28 C. Zhao, X. Jin, X. Jiang, M. Zhou and J. Wei, The chemistry of diacyl peroxides. V. thermal decomposition of pentafluorobenzoyl peroxide in ten different solvents, *Acta Chim. Sin.*, 1986, **44**, 1100–1105.
29 T. Lu, S. L. Liu, Y. H. Sun, W.-H. Wang and M.-X. Pan, A free-volume model for thermal expansion of metallic glass, *Chin. Phys. Lett.*, 2022, **39**, 036401.

30 Y. K. She, S. X. Wang, Q. Liao and M. J. Lin, Transparent and highly organosoluble aromatic polyimides with twisted backbone and bulky side substituents for flexible substrate materials, *J. Polym. Sci.*, 2024, **62**, 1061–1073.
31 W. Lee, J. Kim, H. Hong, H. Noh, D. Park, H. M. Jung and J. Kim, Synthesis of a novel fluorinated polyimide for preparing thermally conductive polyimide composites, *Polym. Compos.*, 2024, **45**, 15915–15923.
32 Y. Shi, J. Hu, X. Li, J. Jian, L. Jiang, C. Yin, Y. Xi, K. Huang, L. Su and L. Zhou, High comprehensive properties of colorless transparent polyimide films derived from fluorine-containing and ether-containing dianhydride, *RSC Adv.*, 2024, **14**, 32613–32623.
33 Z. Chen, Y. Zhang, J. Zhao, Y. Mo and S. Liu, Imparting low dielectric constant and high toughness to polyimide via physical blending with trifluoropropyl polyhedral oligomeric silsesquioxane, *Polym. Eng. Sci.*, 2022, **62**, 2809–2816.
34 W.-F. Peng, H.-Y. Lei, X.-X. Zhang, L.-H. Qiu and M.-J. Huang, Fluorine substitution effect on the material properties in transparent aromatic polyimides, *Chin. J. Polym. Sci.*, 2022, **40**, 781–788.
35 Z. Chen, Y. Zhou, Y. Wu, S. Liu, H. Huang and J. Zhao, Fluorinated polyimide with polyhedral oligomeric silsesquioxane aggregates: Toward low dielectric constant and high toughness, *Compos. Sci. Technol.*, 2019, **181**, 107700.
36 Y. Ji, Y. Bai, X. Liu and K. Jia, Progress of liquid crystal polyester (LCP) for 5G application, *Adv. Ind. Eng. Polym. Res.*, 2020, **3**, 160–174.
37 Q. Yin, Y. Qin, J. Lv, X. Wang, L. Luo and X. Liu, Reducing intermolecular friction work: preparation of polyimide films with ultralow dielectric loss from MHz to THz frequency, *Ind. Eng. Chem. Res.*, 2022, **61**, 17894–17903.
38 S.-Y. Zhang, T. Fu, Y. Gong, D.-M. Guo, X.-L. Wang and Y.-Z. Wang, Design and synthesis of liquid crystal copolyesters with high-frequency low dielectric loss and inherent flame retardancy, *Chin. Chem. Lett.*, 2023, **34**, 107615.
39 H. Dai, Y. Zhang, Y. Yang, J. Chen, C. Li, H. Liu, W. Liu, X. Li, T. Zhang, R. Xue and T. Li, The influence of diamine structure on low dielectric constant and comprehensive properties of fluorinated polyimide films, *Eur. Polym. J.*, 2025, **222**, 113614.
40 Y. Li, Z.-W. Pu, Z.-Z. Yang, Y.-D. Wang, Y.-T. Shen, J.-B. Wu, L. Long, Y.-N. Zhou and W.-C. Yan, Design and synthesis of fluorinated polyimides with low thermal expansion and enhanced dielectric properties, *J. Colloid Interface Sci.*, 2025, **685**, 938–947.
41 X. Lv, S. Qiu, S. Huang, K. Wang, J. Li, Z. He, G. Zhang, J. Lu and R. Sun, A strategy to construct low temperature curable copolyimides with pyrimidine based diamine, *Polymer*, 2022, **261**, 125418.
42 Y.-C. Chen, Y.-C. Lin, E.-C. Chang, C.-C. Kuo, M. Ueda and W.-C. Chen, Investigation of the structure–dielectric relationship of polyimides with ultralow dielectric constant and dissipation factors using density functional theory, *Polymer*, 2022, **256**, 125184.
43 H. Lei, X. Li, J. Wang, Y. Song, G. Tian, M. Huang and D. Wu, DFT and molecular dynamic simulation for the dielectric property analysis of polyimides, *Chem. Phys. Lett.*, 2022, **786**, 139131.
44 J. Lee, S. Yoo, D. Kim, Y. H. Kim, S. Park, N. K. Park, Y. So, J. Kim, J. Park and M. J. Ko, Intrinsic low-dielectric constant and low-dielectric loss aliphatic-aromatic copolyimides: The effect of chemical structure, *Mater. Today Commun.*, 2022, **33**, 104479.
45 C. Zhang, X. He and Q. Lu, High-frequency low-dielectric-loss in linear-backbone-structured polyimides with ester groups and ether bonds, *Commun. Mater.*, 2024, **5**, 55.
46 J. Heo, H. Ahn, J. Won, J. G. Son, H. K. Shon, T. G. Lee, S. W. Han and M.-H. Baik, Electro-inductive effect: Electrodes as functional groups with tunable electronic properties, *Science*, 2020, **370**, 214–219.
47 S. R. Nagella and C.-S. Ha, Structural designs of transparent polyimide films with low dielectric properties and low water absorption: a review, *Nanomaterials*, 2023, **13**, 2090.